



## Patterning of oxide-hardened gold black by photolithography and metal lift-off



Deep Panjwani<sup>a</sup>, Mehmet Yesiltas<sup>a</sup>, Janardan Nath<sup>a</sup>, D.E. Maukonen<sup>a</sup>, Imen Rezadad<sup>a</sup>, Evan M. Smith<sup>a</sup>, R.E. Peale<sup>a,\*</sup>, Carol Hirschmugl<sup>b</sup>, Julia Sedlmair<sup>c,d</sup>, Ralf Wehlitz<sup>d</sup>, Miriam Unger<sup>e</sup>, Glenn Boreman<sup>f</sup>

<sup>a</sup> Department of Physics, University of Central Florida, Orlando, FL 32816, United States

<sup>b</sup> Department of Physics, University of Wisconsin–Milwaukee, Milwaukee, WI 53211, United States

<sup>c</sup> USDA Forest Service, Products Laboratory, Madison, WI 53726, United States

<sup>d</sup> Synchrotron Radiation Center, University of Wisconsin–Madison, Stoughton, WI 53589, United States

<sup>e</sup> Cetics Healthcare Technologies GmbH, Esslingen am Neckar, Germany

<sup>f</sup> Department of Physics and Optical Science, University of North Carolina, Charlotte, NC 28223, United States

### HIGHLIGHTS

- We report the patterning of oxide-hardened gold black with standard photolithography and metal lift-off.
- The minimum pattern length-scale achieved was less than 10  $\mu\text{m}$  after lift-off.
- Average  $\sim 90\%$  absorption in 3–5  $\mu\text{m}$  wavelength window is observed on the patterns.
- For IR array detectors, we provide a method to selectively coat the active regions of individual pixels.
- This method will help improve the sensitivity of current generation micro-bolometers.

### ARTICLE INFO

#### Article history:

Received 19 September 2013

Available online 18 November 2013

#### Keywords:

Gold black

Patterning

MEMS

Photolithography

Infrared

Bolometer

### ABSTRACT

A method to pattern infrared-absorbing gold black by conventional photolithography and lift-off is described. A photo-resist pattern is developed on a substrate by standard photolithography. Gold black is deposited over the whole by thermal evaporation in an inert gas at  $\sim 1$  Torr.  $\text{SiO}_2$  is then deposited as a protection layer by electron beam evaporation. Lift-off proceeds by dissolving the photoresist in acetone. The resulting sub-millimeter size gold black patterns that remain on the substrate retain high infrared absorption out to  $\sim 5$   $\mu\text{m}$  wavelength and exhibit good mechanical stability. This technique allows selective application of gold black coatings to the pixels of thermal infrared imaging array detectors.

© 2013 Elsevier B.V. All rights reserved.

## 1. Introduction

In thermal IR sensors (e.g. bolometers), absorptive coatings convert IR incident power into heat. Many different absorber materials have been investigated, including thin metals, SiN films [1], and metamaterials [2]. Gold black is an absorber that has been used for many decades for IR bolometers [3], particularly for dedicated single-use applications such as space missions. This material achieves nearly unity absorption from visible to far infrared [4–7].

Gold black is a nano-crystalline deposit of gold with extremely low density, low heat capacity, and a refractive index close to unity

[4]. Broader application to commercial array detectors is hampered by its extreme fragility, which also makes it difficult to pattern. In array detectors, only the sensing element should be coated to avoid thermal and electrical bridging between pixels. Laser ablation has been used in the past to remove coatings deposited between the pixels, but this slow process is unsuited to mass production [8].

Stencil lithography has shown some success at patterning gold black, but stencil mask alignment is tedious, the masks must be cleaned between use, and the edges of the resulting patterns are blurry [9]. The patterns we previously reported [9] were hardened with cyanoacrylate using a fuming apparatus, but the heavy polymer chains collapse the gold black film. The resulting loss of porosity and increase in the refractive index caused an unwanted increase in reflection at the top surface. The smallest feature size achieved by us was  $\sim 80$   $\mu\text{m}$ . The Geostationary Earth Radiation

\* Corresponding author. Tel.: +1 4072569884.

E-mail address: [robert.peale@ucf.edu](mailto:robert.peale@ucf.edu) (R.E. Peale).

Budget (GERB) instruments launched by the European Space Agency (ESA) achieved patterned stencil deposition on  $50 \times 50 \mu\text{m}^2$  micro-bolometer pixels, but this gold black was unprotected [10]. In contrast, the new approach presented here using evaporated  $\text{SiO}_2$  over-coating provides hardening and stabilization together with the opportunity to achieve patterned depositions below  $10 \mu\text{m}$  dimensions via standard lift-off.

In usual metal lift-off, a pattern is prepared by spinning photoresist, exposing this layer to UV through a shadow mask, and developing with solvents to open patterned windows down to the substrate. Then metal is deposited over the entire wafer, which is finally submerged in solvent to remove the remaining photoresist and the metal on top of it. The metal stuck to the substrate remains. Lift off can be performed only if the metal adheres strongly to the substrate and if the metal is not attacked by the solvent. None of these conditions is satisfied by usual gold black, which is immediately washed off in the final lift-off step from all areas of the substrate.

Patterning of gold black on infrared focal plane arrays by conventional lift-off was reported in [11]. However, the reported absorption spectrum was clearly stated to be of unpatterned gold black, and so evidently was the SEM image of gold black. No data characterizing the gold black properties after the lift-off procedure were presented. Our experience is that the porous structure necessary to maintain high absorption cannot withstand immersion or saturation in liquid chemicals of any kind for any amount of time, and there remains no clear published evidence to suggest otherwise.

This paper describes the preparation of mechanically-robust, sub-millimeter scale, gold black patterns having nearly 100% absorption out to mid-infrared wavelengths. The approach is by standard photolithography and metal lift-off, which is made possible by mechanically stabilizing the gold black with an evaporated oxide coating.

## 2. Experimental details

Fig. 1 presents a schematic of the deposition process. Negative photoresist NR1500 PY was spin-coated to thickness  $1 \mu\text{m}$  on silicon substrate. A mask pattern was transferred to the resist using an OAI 200 contact mask aligner. RD6 developer was used to remove the unexposed parts, leaving behind bare silicon substrate, which was further cleaned by an oxygen plasma de-scum.

Gold black was deposited following the method of Harris [4–7]. The sample was placed on a temperature-controlled heat sink in a thermal evaporation chamber. The heat sink temperature was maintained at  $-13 \text{ }^\circ\text{C}$  using a Peltier cooler. The chamber was first evacuated to  $10^{-5}$  Torr. Then it was brought to 400 mTorr by continuous controlled flow of nitrogen. Gold wire in the amount 85 mg and of 99.9% purity was placed in a molybdenum boat. The current applied to the boat was 65 A for all depositions. The inert gas causes gold atoms to collide and bind with each other to form web-like structures before landing on the sample.

The instability and fragility of gold black make it incompatible with PECVD oxide deposition due to the high temperatures involved. Instead, we deposited  $\text{SiO}_2$  on the gold black sample by electron beam evaporation. The source was fused silica pellets of 99.99% purity placed in a 7 cc carbon crucible. The chamber was evacuated to  $2 \times 10^{-6}$  mTorr and a wide, high-frequency e-beam sweep pattern maintained a deposition rate of 2–3 nm/s. The thickness of the film and rate of deposition were continuously measured by a quartz crystal monitor (Inficon XTC). The sample was placed normal to the target boat at the optimized distance of 30 cm to keep the temperature below  $60 \text{ }^\circ\text{C}$ . A thermocouple monitored the temperature of the substrate holder during the process. The

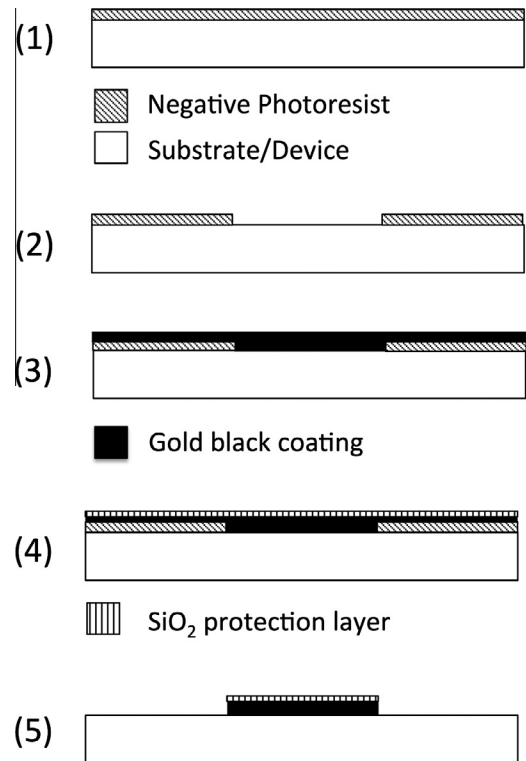


Fig. 1. Schematic of processing sequence patterned gold black/ $\text{SiO}_2$  composites.

$\text{SiO}_2$  film undergoes compressive stress after venting the chamber. The stress reverses to tensile direction logarithmically with time until it reaches a stable state [12]. Therefore, the substrate was kept at atmospheric pressure for more than 10 h to allow it to reach mechanical equilibrium before absorption measurements.

Infrared absorption spectroscopy was performed on gold black with and without  $\text{SiO}_2$  over-coating using a Vertex 80 FTIR equipped with Hyperion 1000 Microscope. The upper aperture in the microscope defines the illuminated sample area, which was chosen to be  $3 \text{ mm}^2$ . For vis–NIR measurements a  $\text{CaF}_2$  microscope objective (2.4 $\times$ , NA 0.07),  $\text{CaF}_2$  beam splitter, tungsten source, and Si diode and mercury–cadmium–telluride (MCT) detectors were used. For the mid-IR range ( $4000\text{--}650 \text{ cm}^{-1}$  range), we used a ZnSe microscope objective (2.4 $\times$ , NA 0.07), Globar source, KBr beam splitter, and 77 K MCT detector. Adequate signal-to-noise ratio was attained by co-adding 128 FTIR scans at  $4 \text{ cm}^{-1}$  spectral resolution.

For IR imaging micro-spectroscopy with high spatial resolution, we used the Infrared Environmental Imaging (IRENI) beam line at the Synchrotron Radiation Center, University of Wisconsin, Madison [13]. A Bruker Vertex FT-IR spectrometer with Hyperion 3000 IR microscope used multiple combined beams of the synchrotron source to provide up to 1000 times higher brightness than available from a globar. A Focal Plane Array (FPA) detector allowed spectral imaging with better than  $1 \mu\text{m}$  spatial sampling. The spectral resolution was  $4 \text{ cm}^{-1}$  and the spectral range was  $900\text{--}3700 \text{ cm}^{-1}$ . For reflectance measurements, the microscope was equipped with 20 $\times$ , 0.65 numerical aperture (NA) Schwarzschild objective. IRidys (Infrared Imaging & Data Analysis) program, which runs on the commercial software package IGOR PRO, was used to extract spectra from different pixels [14].

The fraction of light absorbed by the gold black coating is the absorbance  $A = (1 - T - R)$ , where  $T$  is the transmittance and  $R$  the reflectance. For Vis–NIR, the sample was deposited on an optically thick gold surface, giving  $T = 0$ . For mid-IR measurements, double-sided polished (DSP) silicon was used as the substrate. Bare DSP Si

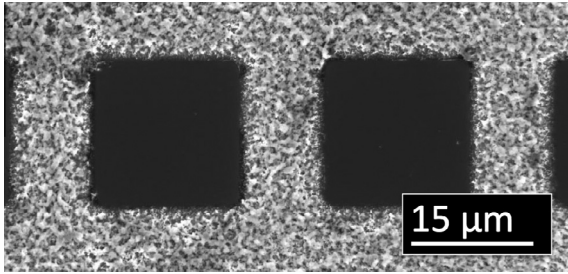


**Fig. 2.** SEM images gold black pattern over-coated with 150 nm SiO<sub>2</sub> on Si substrate. The smallest patterned feature is less than 10 μm.

was used to collect the reference spectra needed for calculation of  $T$ .

Scanning electron microscopy was performed using a Zeiss Ultra-55 SEM. To determine thicknesses, coatings were imaged edge-on. Samples were mounted at 90 deg using carbon tape. The uncertainty in this angle was less than 5 deg, so that the uncertainty in thickness measurements was less than 0.4%.

For four point measurements of resistivity, non-conducting substrates with evenly spaced gold ribbon electrodes were prepared by photo-lithography. The distance between the electrodes was 500 μm, while the average thickness of all gold-black coatings was less than 10 μm. Thus, the sheet resistance is given by [15]

$$R_s = 4.53 V/I, \quad (1)$$

where voltage ( $V$ ) and applied current ( $I$ ) are measured between inner and outer electrodes, respectively.

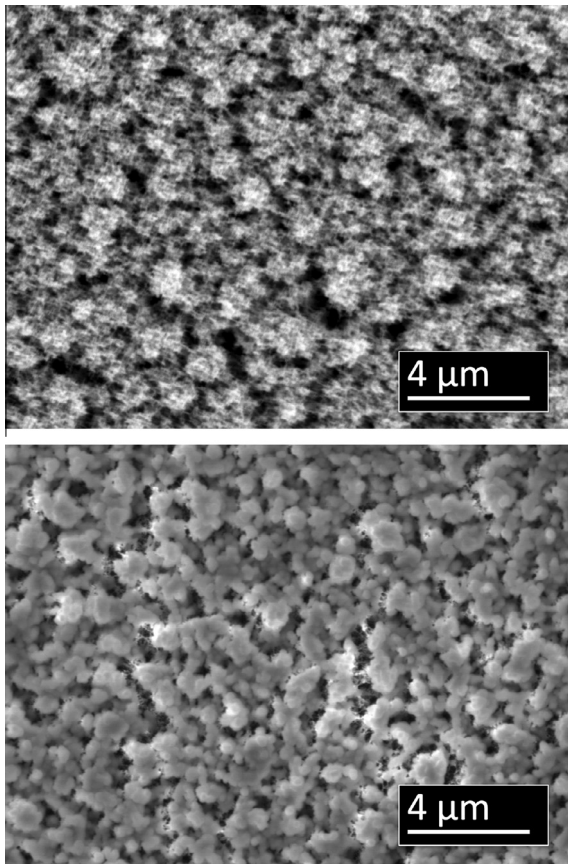


**Fig. 3.** SEM top-view images of gold black coating before (top) and after (bottom) SiO<sub>2</sub> deposition.

### 3. Results and discussion

**Fig. 2** presents an SEM image of a gold black-SiO<sub>2</sub> micro pattern (bright) on silicon substrate (dark). The thickness of the SiO<sub>2</sub> protection layer was optimized at 150 nm. We prepared several different patterns tens of times repeatedly. These exhibited high resistance to mechanical damage. The smallest feature size achieved was close to 9 μm.

**Fig. 3** presents the top view SEM images of gold black coatings before (top) and after (bottom) 150 nm of SiO<sub>2</sub> is deposited. The oxide covers and reduces the roughness of the gold black surface leaving open only the largest of the pores.

**Fig. 4** presents SEM cross-sectional side views of the same region on the same sample, where location is confirmed by features that appear on the substrate. These images indicate that the gold black retains its original 3.5 μm thickness after the oxide over-coating. The large pores near the middle and bottom of the gold black layer retain their size, indicating that the 150 nm thick oxide mainly settles on the surface.

**Fig. 4** also gives the sheet resistance values for this sample, showing little change with oxide deposition.

If the oxide were to compress the film, inter-connectedness would increase, lowering the resistance and potentially changing the IR absorption. Therefore, we again can conclude that the SiO<sub>2</sub> settles lightly on the gold black without compressing it or otherwise altering the structure.

**Fig. 5** presents gold-black absorptance spectra in the visible/near-IR and mid- to long-wave IR wavelength ranges. In the visible/near IR, the absorptance is unity and differs by less than the noise (<~0.2%) before and after oxide deposition and after lift-off.

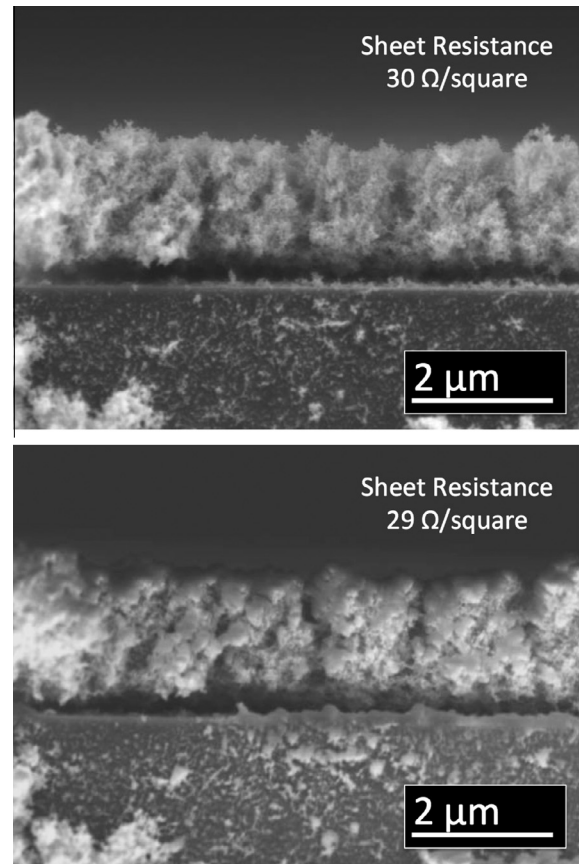


**Fig. 4.** Cross-sectional SEM images of gold black before (top) and after (bottom) SiO<sub>2</sub> deposition.



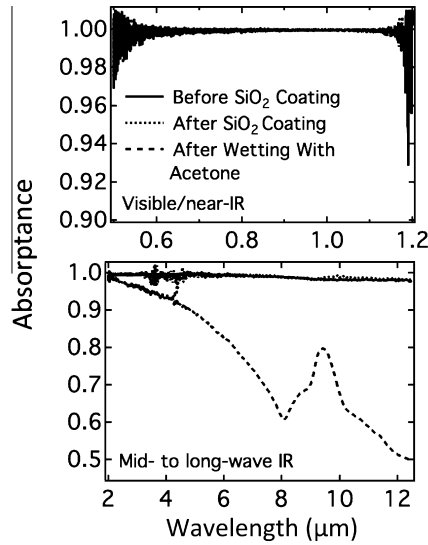


**Fig. 5.** Absorbance spectra for gold black with 150 nm of SiO<sub>2</sub> over-coating. (top) vis–NIR. (bottom) Mid- to long-wave IR.

In the mid- to long-wave IR, the absorbance similarly has the value unity and is indistinguishable before and after oxide deposition. However, after immersion in acetone for 10 s, as occurs during lift-off, the long wave absorbance decreases. Then, it becomes possible to observe an absorption band near 9.4  $\mu\text{m}$  wavelength that we attribute to SiO<sub>2</sub>. Moreover, this treatment caused a decrease in sheet resistance from 30 to 8  $\Omega/\text{square}$ . Though oxide gives considerable protection, acetone apparently

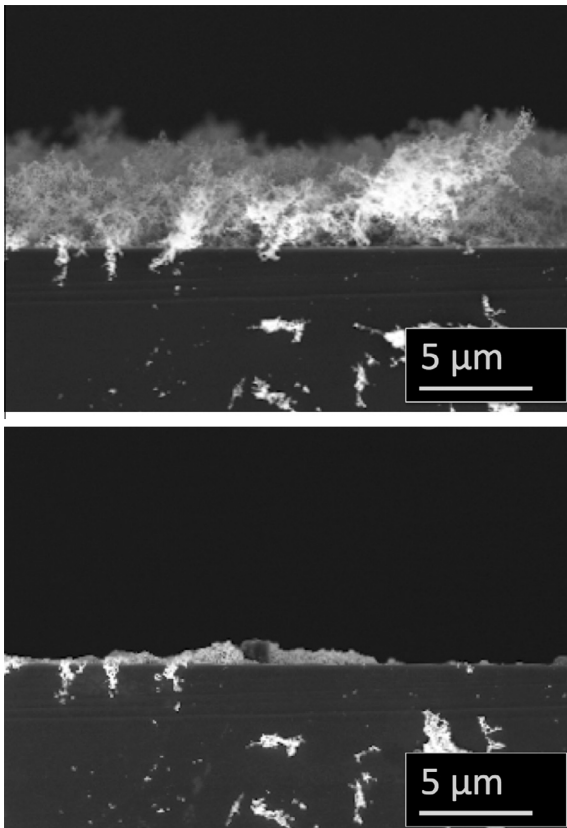
can still pass through the largest pores, causing some morphological change. Even so, the lowest absorbance after lift-off (at 12  $\mu\text{m}$  wavelength) is still 50%.

Fig. 6(top) and (bottom) present cross sectional SEM images of the same region on the same *unprotected* gold black sample before and after immersion in acetone for 10 s. The average thickness of gold black coating was 4.79  $\mu\text{m}$  before wetting, which drastically collapsed the unprotected film to less than 500 nm. Some portion of the coating completely came off from the substrate.

Fig. 7(top) and (bottom) present cross sectional SEM images of the same region on the same *oxide-protected* gold black sample. In contrast to the unprotected case, 10 s immersion caused only a partial collapse, from 8.79 to 2.44  $\mu\text{m}$ . Since  $T=0$ , the reduced long-wave absorbance (Fig. 5) is attributed to increased reflectance due to higher optical density. Reflectivity is still close to zero in the NIR region.

Just 50 nm of oxide enables lift-off patterning, but 150 nm is necessary to preserve significant absorption in the 3–5  $\mu\text{m}$  wavelength atmospheric window. To eliminate the pores, 500 nm of oxide is needed, but then the lift-off is not clean. Such films also crack after venting the chamber, presumably due to compressive stress. Ultrasonic agitation cannot be used to expedite lift-off because it damages the films. Thus, the optimum thickness appears to be 150 nm.

Fig. 8(top) presents an optical microscope image of the region studied by the synchrotron-based IR micro-spectroscopy. The dark region is oxide-protected gold black and the bright region is bare gold substrate. The square in Fig. 8(top) indicates the region of the IR image plotted in Fig. 8(bottom), which is an integrated infrared image in reflectance mode with the scan area of  $\sim 38 \times 43 \mu\text{m}^2$ . This infrared image (bottom) is a mosaic of  $4 \times 3$  tiles, each having



**Fig. 6.** Cross-sectional SEM images of unprotected gold black before (top) and after (bottom) wetting in Acetone.

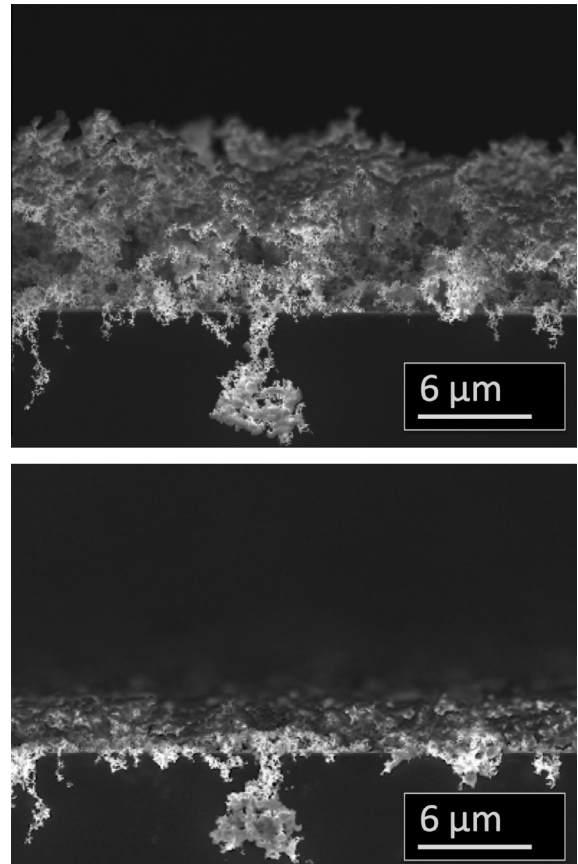


**Fig. 7.** Oxide over-coated gold black before (top) and after (bottom) wetting in acetone.

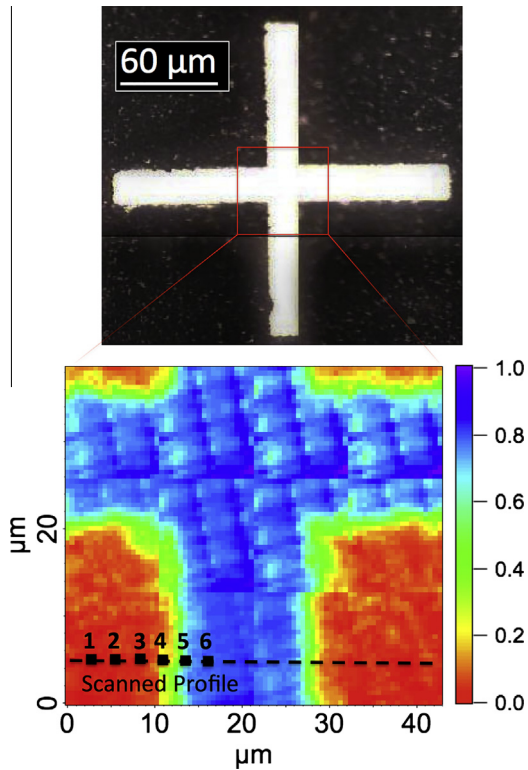


**Fig. 8.** (top) Optical image of photo lithographically patterned gold black with 150 nm of SiO<sub>2</sub> thick protection layer (dark) on gold substrate (bright). (bottom) Integrated infrared reflectance of gold black pattern (900 to 3700 cm<sup>-1</sup>). The infrared image is a mosaic formed by stitching 4 × 3 hyper-spectral tiles.

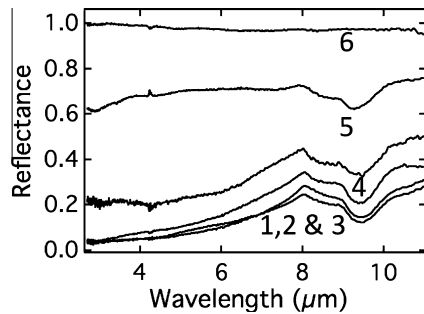


**Fig. 9.** Reflectance spectra extracted from six different pixels shown in Fig. 8.

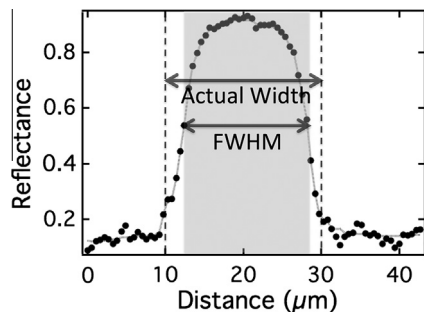


**Fig. 10.** Reflectance line profile across a nominally 20 μm wide oxide-protected gold-black pattern showing decreased absorption at its edges. The dots represent the actual data points and the grey line is obtained from smoothing the data using Savitzky–Golay algorithm as a guide to the eye to calculate FWHM.

~12 × 11 μm<sup>2</sup> area. These tiles are collected one by one, and combined together by the software “OPUS”. There is a small but insignificant bias artifact in the color scale for 2 of the consecutive tiles. The color scale gives the reflectance values, such that the gold black region appears red (high absorbance) and gold substrate appears blue (high reflectance).

Fig. 9 presents reflectance spectra extracted from the six different pixels indicated in Fig. 8(bottom). The reflectance dip at 9.4 μm wavelength is due to the SiO<sub>2</sub> absorption band. The spectra for pixels 1, 2 and 3 are located on the gold black and show less than 10% average reflectance from 3 to 5 μm wavelength. Pixels 4 and 5, which lie in the intermediate reflectance region show higher overall reflectance and a weaker oxide band, showing that the oxide thickness tapers off in this region. Pixel 6 is located on the bare gold-coated substrate and shows the expected 100% reflectance from the gold surface. Similar results over larger areas show that the variation of the gold black absorption is less than 2% over length scales of 42 μm.

The cross pattern in Fig. 8 consist of two perpendicular bars of visible width 20 μm. The reflectance across the line in Fig. 8 is plotted in the graph Fig. 10. The FWHM of this curve is smaller at 15.7 μm than the visible width. This indicates an edge effect, possibly due to greater access for the solvent to the gold-black at the edges of the oxide protection layer. The gradient region of intermediate reflectance in Fig. 8 is represented by green region and it extends over ~2–3 μm distance. This result suggests that the smallest pattern that can retain 100% absorption at its center will be ~10 μm.

#### 4. Conclusion

We reported the patterning of oxide-hardened gold black with standard photolithography and metal lift-off. The minimum pattern length-scale achieved was less than 10 μm. Although SiO<sub>2</sub> coating prevents complete collapse into bulk gold state, a small amount of acetone solvent still passes through SiO<sub>2</sub> pores to damage gold black, which reduces the absorption beyond 2 μm wavelength and degrades it near the pattern edges. Still, these gold black patterns retain more than 90% absorption in the mid-IR (3–5 μm wavelength) range. For IR array detectors, the reported patterning process provides a means to selectively coat the active regions of individual pixels.

#### References

- [1] F. Jutzi, D.H.B. Wicaksono, G. Pandraud, N. de Rooij, P.J. French, Far-infrared sensor with LPCVD-deposited low-stress Si-rich nitride absorber membrane—Part 1, *Opt. Absorp. Sens. Actuators, A* 152 (2009) 119–125.
- [2] Janardan Nath, Douglas Maukonen, Evan Smith, Pedro Figueiredo, Guy Zummo, Deep Panjwani, Robert E. Peale, Glenn Boreman, Justin W Cleary, Kurt Eyink, Thin-film wide-angle design-tunable selective absorber from near UV to far infrared, *Proc. SPIE* 8704 (2013) (87041D–87041D-7).
- [3] Bin Wang, Jianjun Lai, Erjing Zhao, Haoming Hu, Qian Liu, Sihai Chen, Vanadium oxide microbolometer with gold black absorbing layer, *Opt. Eng.* 51 (2012) (074003–074003-6).
- [4] W. Becker, R. Fettig, A. Gaymann, W. Ruppel, Black gold deposits as absorbers for far infrared radiation, *Phys. Stat. Sol. (B)* 194 (1996) 241–255.
- [5] L. Harris, The transmittance and reflectance of gold black deposits in the 15- to 100 μm region, *J. Opt. Soc. Am.* 51 (1961) 80–82.
- [6] L. Harris, R.T. McGinnies, B.M. Siegel, The preparation and optical properties of gold blacks, *J. Opt. Soc. Am.* 38 (1948) 582–589.
- [7] L. Harris, J.K. Beasley, The infrared properties of gold smoke deposits, *J. Opt. Soc. Am.* 42 (1952) 134–140.
- [8] N. Nelms, J. Dowson, N. Rizvi, T. Rohr, Laser micromachining of goldblack coatings, *Appl. Opt.* 45 (2006) 6977–6981.
- [9] Deep R. Panjwani, Nima Nader-Esfahani, Doug Maukonen, Imen Rezadad, Javaneh Boroumand, Evan Smith, Janardan Nath, Robert Peale, Patterning and hardening of gold black infrared absorber by shadow mask deposition with ethyl cyanoacrylate, *Proc. SPIE* 8708 (2013) (870817–870817-8).
- [10] N. Nelms, G. Butcher, O. Blake, R. Cole, C. Whitford, A. Holland, Focal plane array for the GERB instrument, *Proc. SPIE* 5251 (2004) 136–141.

- [11] M. Hirota, Y. Nakajima, M. Saito, M. Uchiyama,  $120 \times 90$  element thermoelectric infrared focal plane array with precisely patterned Au-black absorber, *Sens. Actuator, A* 135 (2007) 146–151.
- [12] Ming. Fang, Hu. Dafei, Jianda. Shao, Evolution of stress in evaporated silicon dioxide thin films, *Chin. Opt. Lett.* 8 (2010) 119–122.
- [13] M.J. Nasse, M.J. Walsh, E.C. Mattson, R. Reininger, A. Kajdacsy-Balla, V. Macias, R. Bhargava, C.J. Hirschmugl, High resolution Fourier-transform infrared chemical imaging with multiple synchrotron beams, *Nat. Methods* 8 (2011) 413–416.
- [14] M.J. Nasse, B. Bellehumier, S. Ratti, C. Olivieri, D. Buschke, Jayne Squirrel, Kevin Eliceiri, B. Ogle, C. Schmidt Patterson, M. Giordano, C.J. Hirschmugl, Opportunities for multiple-beam synchrotron-based mid-infrared imaging at IRENI, *Vib. Spectrosc.* 60 (2012) 10–15.
- [15] Dieter K. Schroder, *Semiconductor material and device characterization*, John Wiley and Sons, New York, 1998.